Yaw-Augmented Control for Wind Farm Power Tracking

Preprint

Genevieve M. Starke,[1] Charles Meneveau,[2] Jennifer King,[1] and Dennice F. Gayme[2]

1 National Renewable Energy Laboratory
2 Johns Hopkins University

Presented at the 2023 American Control Conference
San Diego, California
May 31–June 2, 2023

NREL is a national laboratory of the U.S. Department of Energy
Office of Energy Efficiency & Renewable Energy
Operated by the Alliance for Sustainable Energy, LLC

This report is available at no cost from the National Renewable Energy Laboratory (NREL) at www.nrel.gov/publications.

Contract No. DE-AC36-08GO28308

Conference Paper
NREL/CP-5000-85402
July 2023

Yaw-Augmented Control for Wind Farm Power Tracking

Preprint

Genevieve M. Starke,[1] Charles Meneveau,[2] Jennifer King,[1] and Dennice F. Gayme[2]

1 National Renewable Energy Laboratory
2 Johns Hopkins University

Suggested Citation
Starke, Genevieve M., Charles Meneveau, Jennifer King, and Dennice F. Gayme. 2023. *Yaw-Augmented Control for Wind Farm Power Tracking: Preprint*. Golden, CO: National Renewable Energy Laboratory. NREL/CP-5000-85402. https://www.nrel.gov/docs/fy23osti/85402.pdf.

Conference Paper
NREL/CP-5000-85402
July 2023

National Renewable Energy Laboratory
15013 Denver West Parkway
Golden, CO 80401
303-275-3000 • www.nrel.gov

NOTICE

This work was authored in part by the National Renewable Energy Laboratory, operated by Alliance for Sustainable Energy, LLC, for the U.S. Department of Energy (DOE) under Contract No. DE-AC36-08GO28308. Funding provided by the U.S. Department of Energy Office of Energy Efficiency and Renewable Energy Wind Energy Technologies Office. The views expressed herein do not necessarily represent the views of the DOE or the U.S. Government. The U.S. Government retains and the publisher, by accepting the article for publication, acknowledges that the U.S. Government retains a nonexclusive, paid-up, irrevocable, worldwide license to publish or reproduce the published form of this work, or allow others to do so, for U.S. Government purposes.

Cover Photos by Dennis Schroeder: (clockwise, left to right) NREL 51934, NREL 45897, NREL 42160, NREL 45891, NREL 48097, NREL 46526.

Yaw Augmented Control for Wind Farm Power Tracking

Genevieve M. Starke[1], Charles Meneveau[2], Jennifer King[1] and Dennice F. Gayme[2]

Abstract— **This paper presents an inner-outer control loop structure which uses wake steering (yaw control) to augment pitch control for wind farms to track a power reference signal. The outer-loop yaw controller employs a recently proposed dynamic yaw model with a time-varying graph structure that accounts for dynamic changes in the farm wake interactions due to the yaw action of upstream turbines. The wake interactions within the model include the physics of the streamwise and lateral wake evolution, which collectively determine its impact on downstream turbines. The inner-loop employs a compensation scheme to account for the slow timescale effects of the yaw control actions within the faster timescale pitch control. The controller is applied to track two power trajectories (typical of secondary frequency regulation signals) using a large eddy simulation wind farm plant. The results demonstrate that the additional control authority from yaw provides some added benefit in reducing the required turbine derates needed for wind farms to track transient power increases in the proposed setting. However, the benefit decreases and pitch control alone is sufficient when the turbines are derated beyond a certain level. These findings suggest that augmenting pitch control with yaw may provide financial incentives in terms of allowing wind farms to maximize power supply to the bulk power market while still providing regulation services. Further work is needed analyze the costs versus benefits of the additional control complexity versus bandwidth in augmenting pitch control with wake steering offers in these applications.**

I. INTRODUCTION

Wind energy is rapidly growing worldwide. For example, in the US the electricity supplied by wind has grown from 2.9% to 9.2% over the last 10 years [1] and offshore wind is poised to accelerate this already steep growth rate. As wind energy becomes more prominent, it becomes increasingly important to enable not only efficient stand alone operation but also integration with the electricity grid. Ancillary services play an important role in maintaining the reliability of the grid, particularly in maintaining the required supply/demand power balance. Secondary frequency regulation is one such service that both individual wind turbines and wind farms can provide, see e.g. [2], [3], [4], [5] and references therein.

At the turbine level, tracking a power signal requires derating (reducing the power setpoint of the turbine from the maximum level) in order to provide additional power to track upward trends in the power trajectory. At the farm level wake interactions become particularly important as the wake propagation through the farm is on a similar timescale as regulation [6]. Failing to account for these interactions can result in the inability to control the overall farm flow [7]. Researchers have accounted for these interactions in a number of ways when controlling high-fidelity simulation based plant models (e.g. large eddy simulations). For example, Proportional-Integral (PI) controllers at the turbine level were coordinated to enable wind-farm level control [4] where derating of the turbines was used to overcome the wake effects. Shapiro et al. instead employed a model-based receding horizon controller using a model that took into account the advection of the wake using an one dimensional advection-diffusion model [6]. Their approach enabled power tracking at lower derates with performance that would allow qualification in the PJM[1] secondary frequency regulation market [8].

While effective and robust control can be achieved through higher derates, this may be undesirable from a wind farm operator perspective as they will lose revenue in the bulk power market. The increased pitching used to implement derates in practice could lead to larger turbine loads. A number of studies have sought to overcome the latter issue by co-optimizing blade loading and power tracking [9]. There are also algorithms that offer a distributed framework and also attempt to minimize the loads on the turbines in the farm [10] or maximize the available power while following a signal [11]. Many of the current power tracking control approaches employ the thrust coefficient, which would be implemented using generator torque or blade pitch control [12]. Another approach is to find additional actuation authority that does not require derating the turbine, such as is yawing actuation.

Yaw control, or wake steering, has generated considerable recent interest as a means of increasing wind farm power output [13], [14], [15]. Increasing the overall output of the wind farm through yawing has been demonstrated in simulations [16], [13], experiments [17], [14], and more recently in field tests [18], [19], [15], [20]. To date the focus has been on power maximization rather than trajectory tracking control. The approaches and settings have varied, such as a heuristic wake model or LES to generate set points for the yaw controller [19]. Steps have also been taken to account for the inter-turbine propagation time of wakes in for example setpoint optimization using a model free approach in a wind tunnel test [21] and using time delays in a field test [22]. Recent work has sought to apply yaw control in power tracking applications. For example, it was applied in one study using a linear model derived from data [23]. Although this approach showed promise, such an approach would be

[1] Genevieve M. Starke and Jennifer King are with the National Wind Technology Center, National Renewable Energy Laboratory, Golden, CO 80401, USA; email: Genevieve.Starke@nrel.gov, Jennifer.King@nrel.gov.

[2] Charles Meneveau and Dennice F. Gayme are with the Department of Mechanical Engineering, Johns Hopkins University, Baltimore, Maryland 21218, USA; email: meneveau@jhu.edu, dennice@jhu.edu

[1] PJM is an independent system operator in the US

less suitable under changing wind conditions as such a model would need to be re-derived for any perturbation in the inflow.

The potential of combining yaw with control of the thrust coefficient was explored in the context of maximizing power output using a high-fidelity (large eddy) simulation [24]. They found gains of $25\% - 34\%$ in the power output using a large eddy simulation (LES) model-based receding horizon control to control a LES wind farm. While illustrative of the benefits of using a model with full knowledge (or as close to it as one can get in a simulation), the use of LES as the model in the controller means that computation of the control actions cannot be carried out in real-time. The work by Boersma et al. [3] took an important step toward integrated yaw and pitch control using model predictive control for both the inner pitch and outer control loops. The yaw actuation was only active in instances where the pitch control was unable to track the power reference signal. They employed static yaw configurations that were computed every 15 minutes. Their controller demonstrated strong tracking performance with the turbines derated to 70 or 80% of the full power available.

This work seeks to build upon the previously demonstrated yaw studies in the following ways. In order to implement a combined yaw-pitch control strategy for power tracking, we use an optimization based control of the yaw angles that employs a recently developed dynamic yaw model that enables us to capture the transient response of the yaw actions that were not taken into account in previous work based on static yaw configurations [25]. The control also takes into account the physical rate at which a turbine can yaw by including a rate limit for the yaw actuation. The inner pitch control loop uses a PI controller combined with a novel power sharing arrangement that reduces the needed derate at each turbine. We also propose a pitch-yaw control correction to increase the effectiveness of the pitch control when it is applied in conjunction with the yaw commands. The combined PI control for pitch and model-based yaw optimization using the dynamic yaw model allows real-time control. This integrated control strategy is applied to control an LES wind farm plant in a power tracking application with a range of different turbine derates. The results indicate that while the yaw provides slight improvement over pitch only control in most cases the rate at which the turbine can yaw makes it less beneficial for fast ramping signals. The true benefit of augmenting the pitch with yaw control is observed in the zero derate case as the yaw enables the controller to track the signal in cases where pitch does not have sufficient actuation authority. While future work is needed to fully evaluate and characterise the robustness of this behavior the results here indicate that augmenting a pitch control with yaw could reduce the opportunity cost of wind farms participating in ancillary service markets.

The remainder of this paper is organized as follows. In Section II we present the yaw and pitch controller formulation. Section III includes the wind farm plant setup and the controller performance results. Finally, Section IV presents the conclusions of the paper.

II. The Yaw and Pitch Controller

This section details the design of the control scheme for the wind farm. In Section II-A, we present the problem formulation of the power tracking problem. In Section II-B, we detail the pitch controller design in Section II-B.1 and the yaw controller design in Section II-B.2

A. Power Tracking Problem Formulation

In the power tracking problem, the goal is to minimize the difference between the trajectory (desired wind farm power time series), denoted here as the power reference signal $P_{\text{ref}}(t)$, and the actual power output of the wind farm $P_{\text{WF}}(t)$, where t is time. The problem can be characterized as solving the minimization problem

$$\min_{\gamma} \left[\int_0^{T_a} [P_{\text{WR}}(t; C'_{\text{T}}, \gamma) - P_{\text{ref}}(t)]^2 dt \right], \tag{1}$$

where the power of the wind farm depends on the set of yaw angles γ of all of the wind turbines and the local coefficients of thrust C'_{T} that are determined by the inner loop PI controller for the pitch over the time horizon T_a.

The power reference signal is represented in the form $P_{\text{ref}}(t) = [1 - \alpha_d + r(t)]P_{\text{base}}$, where P_{base} is the average power of the wind farm in the five minutes preceding the start of the control simulation. The time dependent part of the power reference signal $r(t)$ represents the demands of the grid in an active power control situation (which is the power supplied to the bulk market). The parameter α_d is the percentage base power reduction (derate) implemented to allow the tracking of ramping in the reference signal. This derate represents a loss in revenue for the wind farm, since the power that is available for sale in the bulk power market is being reduced. A goal in this work is to maximize the control authority, while also minimizing the derate necessary to track the signal.

B. Controller Framework

We combine the yaw and pitch controllers by separating the control framework into an inner loop for pitch control and an outer loop for yaw control. Figure 1 shows a block diagram of the controller, where the model-based optimal control yaw loop is shown in purple, and the pitch PI loop is shown in teal.

1) Pitch Controller: The PI control is based on wind turbine power feedback, which is used to calculate a pitch update to adjust the thrust coefficients of the wind turbines. For the i^{th} turbine, the pitch update has the form

$$\Delta C'_{\text{T},} = \text{k}_\text{p} e_{\text{P},i}(t) + \text{k}_i \int_{T_{\text{k}_i}} e_{\text{P},i}(\tau) d\tau + \Delta C'_{\text{T},i,\Delta\gamma}, \tag{2}$$

where k_p is the proportional control gain, k_i is the integral control gain, $e_{\text{P},i} = P_i - P_{\text{ref},i}$ is the error between the power reference signal and the current LES power for turbine i, and T_{k_i} is the timescale of the integral control. We describe our method to relate $P_{\text{ref},i}$ to the prescribed wind farm reference signal P_{ref} after describing the other terms in the equation.

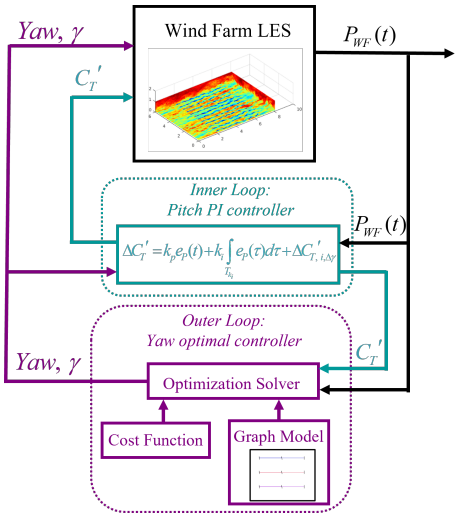

Fig. 1. A block diagram that shows the structure of the model-based optimal control of the wind farm. The outer loop portraying the model-based optimal yaw controller is shown in purple and the inner loop portraying the pitch PI controller is shown in teal.

The quantity $\Delta C'_{\mathrm{T},,\Delta\gamma}$ represents the change in the thrust coefficient required to keep the power constant if the yaw changes for turbine i. This feed-forward pitch correction enables the control law to account for the change in yaw as it happens. Here we replace the true value with the following linearized approximation:

$$\Delta C'_{\mathrm{T},,\Delta\gamma} \approx \frac{d\,C'_{\mathrm{T},}}{d[\cos(\gamma_i)]}\left[\cos(\gamma_{2,i}) - \cos(\gamma_{1,i})\right], \tag{3}$$

where $\gamma_{1,i}$ and $\gamma_{2,i}$ are the original yaw and the final yaw of turbine i, respectively. These are known from the yaw controller output, which is fed into the pitch controller, as shown in Fig. 1.

In order to determine $dC'_{\mathrm{T}}/d[\cos(\gamma)]$ we use the equation for the power of at turbine i: $P_i = \frac{1}{2}C_{P,i}\rho A U^3_{\infty,i}$. Here, ρ is the air density, A is the swept rotor area, $C_{P,i}$ is the power coefficient of turbine i, $U_{\infty,i}$ is the upstream velocity at turbine i. Rearranging this expression and writing the power coefficient in terms of the "local" thrust coefficient C'_{T} (i.e. the thrust coefficient defined in terms of the local rotor disk velocity rather than the free-stream velocity) leads to

$$\frac{2P_i}{\rho A U^3_{\infty,i}} = C'_{\mathrm{T},}\cos^3(\gamma_i)\left(\frac{C'_{\mathrm{T},}}{4+C'_{\mathrm{T},}}\right). \tag{4}$$

We now take derivative with respect to $\cos(\gamma)$, and solve for $dC'_{\mathrm{T}}/d[\cos(\gamma)]$ while requiring that the left-hand side of Eq. 4 does not change with $cos(\gamma)$ (since we are seeking to quantify how the thrust coefficient has to change with yaw angle while maintaining constant power) and obtain

$$\frac{d\,C'_{\mathrm{T},}}{d[\cos(\gamma_i)]} = \frac{-3C'_{\mathrm{T},}(C'_{\mathrm{T},}+4)}{\cos(\gamma_i)(C'_{\mathrm{T},}+16)}. \tag{5}$$

This linearized approximation is determined to be reasonably accurate, with an error below 2.5% within a change in yaw angle of $\pm 1^\circ$, which is the range over which this correction will be applied.

The pitch control law in (2) requires turbine-specific power set points. Since we are only given a total power reference signal for the farm we need a strategy for determining how to distribute this signal to the individual turbines without degrading the overall performance. This is a challenging problem because the fraction of the power provided to the total power from each turbine varies according to the incoming velocity and the relative position of the turbine in the farm. To provide a practical approach that can be implemented easily, we use a model-free, data driven method that measures the fraction of power generated by each turbine in the wind farm over some past time interval and uses that fraction to distribute the reference power to each turbine. Specifically, we use the following expression to determine the reference power for each turbine:

$$P_{\mathrm{Ref},i}(t) = \frac{\int_{t-T_{C'_{\mathrm{T}}}}^{t} P_i(\tau)d\tau}{\int_{t-T_{C'_{\mathrm{T}}}}^{t} P_{\mathrm{WF}}(\tau)d\tau}\; P_{\mathrm{Ref}}(t), \tag{6}$$

where $P_{\mathrm{Ref},i}$ is the resulting individual power reference signal for the i^{th} turbine, $T_{C'_{\mathrm{T}}}$ is the time between pitch controller updates, P_i is the power for the i^{the} turbine in the wind farm (in our application from LES), P_{WF} is, as before, the total wind farm power, and P_{Ref} is the prescribed total power reference signal. Since we take the average over the update time period, this could bias the sum of the distributed turbine-specific power reference signals, however we have verified that the error between the total power reference signal and the sum of the individual power reference signals in our tests was less than 1%.

2) Yaw Controller: The yaw controller uses a model-constrained optimal control framework to determine the yaw commands for each turbine over a finite look-ahead time period. The outer loop yaw control uses a model-constrained optimal control based on (1) constrained by the dynamic yaw model introduced in [25]. This model represents the wind farm as a graph, where the turbines are the nodes of the graph and the interactions between the turbines are the edges of the graph. This approach has the benefit of being computationally efficient and also being able to represent dynamic changes in the state of the wind farm, such as dynamic yawing, which are particularly relevant in this work. The control is implemented in a receding horizon fashion where the yaw angle changes for each turbine in order to optimize performance over the entire optimization time horizon (look ahead period). This look ahead period includes the transient response predicted by the yaw model, which also informs the control actions. These actions are updated based on the current system conditions at a faster yaw control update rate.

The controller uses the Dynamic Yaw model to represent the effect of yaw actions on the wind farm. This model has the form

$$\Phi_{k+1} = A\;\Phi_k + E_k, \tag{7}$$

where Φ represents the state of the system, consisting of all the relevant pairwise turbine interactions as described by the wake velocity deficit caused by upstream turbines, A is the state update matrix, and E is the input to the system. In this model, we use $A = I$, and the state updates are input through E, which describes changes in the relationships between the states of the system, i.e. changes in the turbine interactions (velocity deficits) in the farm.

The states are determined using the following definition of the normalized wake deficit [26]

$$\frac{\delta u}{U_\infty} = C(x)\exp\left[-\frac{(y-y_c)^2+(z-z_h)^2}{2\sigma(x,\theta)^2}\right], \tag{8}$$

where δu is the wake deficit velocity at position (x,y,z), x is the distance to the wake generating turbine, U_∞ is the freestream velocity, $C(x)$ is the initial velocity deficit at the wake center, which is described later, y_c is the y-location of the center of the wake, z_h is the turbine height, and $\sigma(x,\theta)$ is the radial spread of the wake which for yawed turbine wakes can be a function of both streamwise distance x and polar angle θ (i.e. non-axisymmetric wake velocity distribution). A more complete description of the model parameters are provided in [25], while only the main equations of the model are provided in this paper.

The analytical description of the wake deformation due to yaw is represented as

$$\sigma(x,\theta) = k_w x + 0.4\xi(x,\theta), \tag{9}$$

where k_w is the wake expansion coefficient, and ξ is the non-dimensional wake radius for which an analytical description was recently developed [26] for application to yawed turbine wakes.

The initial wake deficit $C(x)$ is calculated using the following equation

$$C(x) = 1 - \sqrt{1 - \frac{C_T \cos^3(\gamma)}{2\tilde{\sigma}^2(x)/R^2}} \tag{10}$$

where C_T is the (standard) thrust coefficient of the turbine, and $\tilde{\sigma}^2$ uses a simplified version of Eq. 9 for computational efficiency to avoid a dependence on θ.

The system state vector at time k

$$\Phi_k = \begin{bmatrix}\phi_1^1 & \phi_1^2 & \phi_1^3 & \dots & \phi_1^N & \phi_2^1 & \dots & \phi_N^{N-1} & \phi_N^N\end{bmatrix}^T, \tag{11}$$

is formed by assembling mean wake deficit velocities ϕ_i^j corresponding to pairs of interacting turbines evaluated at time k. Specifically, each ϕ_i^j is defined as the average of the wake defect velocity for a wake caused by the j^{th} turbine interacting with a downstream turbine i. It is evaluated from the model wake velocity according to

$$\phi_i^j = \frac{1}{A_i}\int_{A_i} C(\Delta x_{i,j})\times \exp\left[-\frac{(y-y_{c,j})^2+(z-z_{h,j})^2}{2\sigma(\Delta x_{i,j},\theta_j)^2}\right] dydz, \tag{12}$$

where A_i is the rotor disk area of the ith turbine and $\Delta x_{i,j} = x_i - x_j$ is the streamwise distance between turbine i and j. The polar angle θ_j in the wake due to turbine j can be computed from $\arctan[(z-z_{h,j})/(y-y_{c,j})]$. The state vector (at time k) Φ_k for a wind farm with N turbines thus has a total of N^2 states.

The system update is determined by the input

$$E_k = f(\Phi_k, \tau_k, \Delta\mathscr{O}_k), \tag{13}$$

which provides the new states, the changes in edges of the wind farm graph as part of the graph-based model, and changes in the time delay inherent to the system. The time delay represents the finite time that is necessary for information to travel between turbines, since aerodynamic information, such as a change in yaw, can only travel between the turbines at the speed of the wind velocity. This quantity is represented by $\tau_i^j = \Delta x_i^j / u_j$ where $\Delta x_i^j = x_i - x_j$ is the distance between the two turbines and u_j is the advection velocity of the flow.

The output of the model is a normalized cumulative deficit coefficient for each turbine Δu_i^*, which is calculated using a delay-dependent adjacency matrix of the graph that describes the current turbine interconnections, according to

$$\Delta u_{k+1}^* = \Lambda(\tau_k)\,\Phi_k(\tau_k). \tag{14}$$

The total deficit coefficient for turbine i is then used to find the disk velocity of turbine i at time $k+1$ from

$$u_{d,i,k+1} = U_{i,\infty}\cos(\gamma_{i,k+1})\left(1-\Delta u_{i,k+1}^*\right)\left(1-\frac{C'_{T,}}{4+C'_{T,}}\right).$$

The disk mean velocity is used to calculate the power from wind turbine i using

$$P_{i,k} = \frac{1}{2}\pi R^2 \rho\, C_P\,(u_{d,i,k})^3\,[cos(\gamma_i)]^p, \tag{15}$$

where for our case we have set $C_P = C_T$. The exponent p determines the effect of yaw on the power and changes for different turbines. The range for p is generally $0.5 \le p \le 2$. This value is typically derived from the specific turbine, and in our study we used a value of $p = 0.5$

The optimal control is implemented by finding the best single value solution to the problem posed in (1) for each turbine over a finite look-ahead period. Since the problem is nonlinear, the optimization is challenging. In this work, we use Powell's algorithm to find the solution of the minimization [27], [28], [29]. Since the solution is sensitive to the initial conditions, we use the average of an ensemble of initial conditions to determine the next yaw step.

III. Power Tracking Results

A. Controller Testing Setup

The pitch-yaw controller was tested on an eighteen-turbine wind farm, whose geometry consists of three columns of six turbines each. The chosen arrangement is consistent with a number of prior studies [6] that focused on aligned regular arrays of wind turbines. The simulations are performed using the JHU LESGO code [30], using the concurrent precursor inflow method [31], the Lagrangian-averaged scale dependent subgrid scale model [32], and actuator disk wind

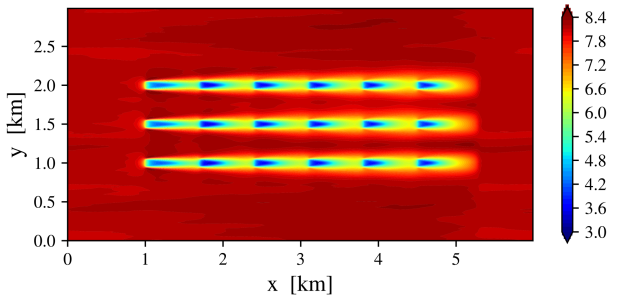

Fig. 2. Average velocity on a horizontal plane at hub-height from an LES of the eighteen-turbine wind farm used in the present control study. The colorbar shows the values in m/s.

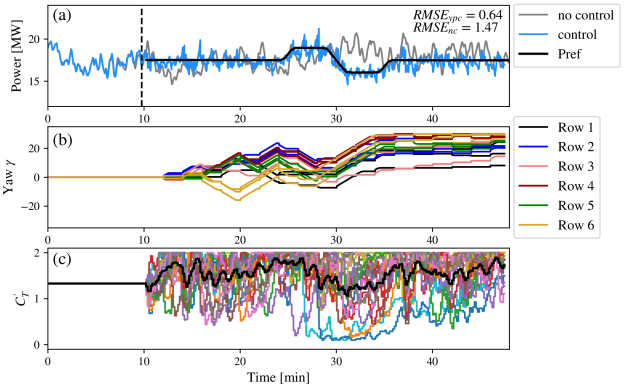

Fig. 3. Results from applying the yaw and pitch controller to an eighteen-turbine wind farm LES plant. The figure shows (a) a comparison between the power reference signal, the LES if no control was applied, and the controlled LES results, (b) the time history of the yaw control, where each row is represented by the same color, and (c) the time history of the coefficient of thrust for each turbine, while the average is shown by the heavy black line.

turbine models [33], [34]. The domain extends $6 \times 3 \times 1$ km in the streamwise, spanwise, and vertical directions with $512 \times 256 \times 192$ grid points in these directions, respectively. The friction velocity is set to be $u_* = 0.45$ m/s and the surface roughness height is specified as $z_0 = 0.1$ m. The turbines have a rotor diameter of $D = 100$ m, a hub height of $z_h = 100$ m, and a local thrust coefficient of $C_T' = 4/3$. An average velocity field from this LES of a wind farm plant is shown in Fig. 2.

Three power reference signals are used to evaluate the control. The first is a sample power reference signal used in previous active power control studies [6] that is designed to integrate to zero. The other two signals are "RegA" and "RegD" signals, which are types of secondary frequency regulation signals used by PJM, the independent system operator (ISO) in the United States Eastern Interconnection. These signals are based on the area control error (ACE) signal. The RegA signal is a low pass filter of the ACE that is usually followed using conventional regulating resources. The RegD signal is a high-pass filter of the ACE and is typically followed by more responsive energy sources such as energy storage devices [8]. RegD signals are also designed to integrate to zero, meaning that there is no net increase or decrease over the entire signal.

In the implementation of the yaw controller, the yaw control is updated every 120 seconds, and the look-ahead time horizon used is 300 seconds. Over the two minute interval, the turbines are yawed according to the set yaw rate, until either they reach the desired yaw, or it is time for another controller update. Since we are performing a nonlinear optimization, an ensemble of optimizations are run (we here used 10 members in the ensemble), each with differing initial conditions that are perturbed randomly within $\pm 2^\circ$ from the current yaw. The final yaw control commands use the average of the ensemble results [35], [25].

The PI controller gains were tuned using the full yaw and pitch controller. We performed both a proportional and integral gain study. The proportional gain was tested at increasing values until the trajectory exhibited worsening oscillations rather than an improved performance. The success of the power tracking is measured using the root mean square error (RMSE) of the signal, calculated as

$$RMSE = \sqrt{\frac{1}{N_{ST}} \sum_{k=1}^{N_{ST}} \left(P_{\mathrm{WF},k} - P_{\mathrm{Ref},k}\right)^2}, \qquad (16)$$

where N_{ST} is the number of measurements taken over the timeframe the control is applied, $P_{\mathrm{WF},k}$ is the total wind farm power from the LES at time k and $P_{\mathrm{Ref},k}$ is the power reference signal value at time k. The chosen PI controller parameter settings from this study to be used in the rest of the results for this section are $\mathrm{k}_p = 1$ and $\mathrm{k}_i = 0.05$. More information on the PI tuning process is available in [35].

B. Simulation Results

Figure 3 shows an example of the control applied to the LES wind farm plant. Figure 3(a) shows the total power of the wind farm, compared with the given power reference signal and the power output of the wind farm if it was run without any control at a constant coefficient of thrust and zero yaw. In the total power plots, the control is turned on after the vertical black dashed line (located at 10 minutes). In the case shown in Fig. 3, $\alpha_d = 0.04$, corresponding to a 4% power derate from the regular operating conditions. We see that the controlled case is able to track the signal both when it requires more power than the uncontrolled case (minutes $25-30$), and also when it requires less power (minutes $30-35$). In the top right corner of Fig. 3(a), we also indicate the RMSE of both the controlled and the uncontrolled signal. Here, the controlled signal has an error that is less than half that of the uncontrolled case.

In addition to the total power, we can also examine the control signals. Figure 3(b) shows the time series of the yaw angle γ of the wind turbines throughout the controlled time period. The turbines are grouped according to row with each row designated by a different color. In this application of the controller, the average of an ensemble of five optimizations was used to determine the yaw control. All the turbines are

initialized at zero yaw and become active after the control is initiated. It can also be seen from this plot that the yaw evolution is limited by the imposed finite yaw rate (namely 4°/min), which determines the ramping behavior that starts around the 30^{th} minute, where the turbines are yawed over several yaw updates.

Fig. 3(c) shows a time history of the coefficient of thrust over the control period. The coefficients of thrust have an initial value of $C'_T = 4/3$, imposed to represent standard operating conditions of the farm before control actions (even though this value is not the maximum allowable value that could be used in a greedy control which refers to control strategies when all of the turbines are attempting to extract the maximum power – in this case by setting the thrust coefficient to the maximum value $C'_T = 2$ independently of the collective wind farm behavior). The different turbine signals are denoted by different colors in Fig. 3(c). The black line denotes the average thrust coefficient, which can be used to determine how much pitch actuation is available in the farm at any given time. The three quantities shown in Fig. 3 characterize the behavior of the yaw and pitch controller as function of time.

In Section II, we outlined how a pitch feed-forward control was implemented to mitigate the effect of the yaw changes on the pitch control. Figure 4(a) shows the behavior of the pitch correction term and and Fig. 4(b) shows the yaw actions that are being accounted for by the pitch feed-forward method, for two representative turbines, namely the second turbine and the sixth turbine (which are in the the second row and sixth row, respectively). One thing to note about this term is that regardless of the sign of the current yaw of the turbine, the compensation term is positive if the yaw is moving away from zero and negative if the yaw is moving towards zero. Since the power will reduce if the turbine is yawed further from the zero yaw position, the coefficient of thrust should be increased to keep the power steady. The effect is reversed if the turbine is yawed closer to zero yaw. This behavior is reflected in the Fig. 4, where the positive sections of the compensation term in Fig. 4(a) correspond to the yaw of the turbine moving further from the zero yaw position, and the negative section in Fig. 4(a) correspond to the yaw of the turbine moving closer to the zero yaw position in Fig. 4(b).

1) RegA and RegD Control Case: In this section we investigate the performance of the controller when applied to a RegA and a RegD signal, and compare the performance of the yaw plus pitch controller with the performance of a controller only using pitch control.

The controller was applied to one RegA and one RegD test signal, and the control was implemented with three different derates (0%, 2%, and 4%) for each signal. Both test signals are 40 minutes long. Further details regarding these signals are provided in [8]. The performance of the yaw plus pitch controller was compared to the uncontrolled LES case and the LES case where only the PI pitch controller was applied and all turbines remained unyawed. Figure 5 shows the total power from these simulations, where grey denotes the uncontrolled LES case, blue denotes the yaw and pitch

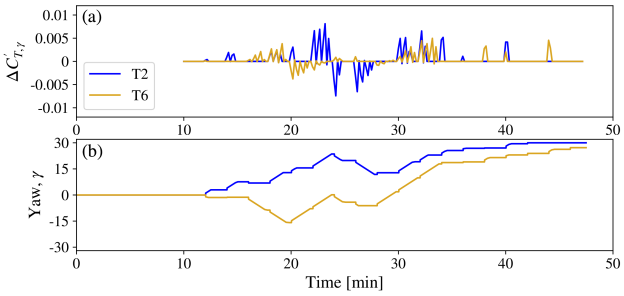

Fig. 4. An example of the pitch compensation for the yaw changes prescribed by the controller in the simulation shown in Fig. 3, where (a) shows the changes in the coefficient of thrust in reaction to the yaw changes, and (b) shows the yaw of a turbine (T2) in the second row and a turbine (T6) in the sixth row.

controlled LES case, red denotes the only pitch controlled LES case, while black represents the power reference signal. The black vertical dashed line shows where the control is initiated in the tests. The type of signal is denoted in the upper left corner, followed by the derate value, where "D0" denotes a 0% derate, and so on. Qualitatively, the yaw plus pitch control performs similarly to the only pitch control, with perhaps smaller fluctuations in some portions. Notably, in the inital portion of the control (from 10-20 minutes), both of the controllers perform very similarly. In this region the pitch control is dominant due to the time delay that is inherent in the yaw control. Since the pitch control in both controllers is the same, the resulting total power from the wind farm is very similar. Once the yaw control becomes more present in the control, which takes approximately 5-10 minutes, the controlled signals from the two cases differ.

Signal Type	4% derate		2% derate		0% derate	
	Yaw + Pitch	Pitch	Yaw + Pitch	Pitch	Yaw + Pitch	Pitch
RegA	0.90	0.82	0.84	0.85	0.90	0.93
RegD	0.82	0.84	0.85	0.92	0.97	1.01

TABLE I

ROOT MEAN SQUARE ERROR OF WIND FARM POWER (IN MW), COMPARING POWER SIGNALS FROM THE CONTROLLED LES PLANT TO THE PRESCRIBED REGA AND REGD TEST SIGNALS.

Quantitatively, we can use root mean square error (RMSE) to compare the difference between the power signals from the controlled LES plant and the reference signals when using either the yaw and pitch controller or the only pitch controller. The RMSE for each of these cases is shown in Table I. The average RMSE for the yaw and pitch controller for these six cases is 0.88, and the average RMSE for just the pitch control is 0.90, slightly higher. We can see that the yaw and pitch control performs slightly better than just the pitch control for all cases except the RegA with 4% derate. This is associated with the dip in the total power for the yaw and pitch control visible around minute 35 in Fig. 5 for this case. This dip is a combination of yaw being

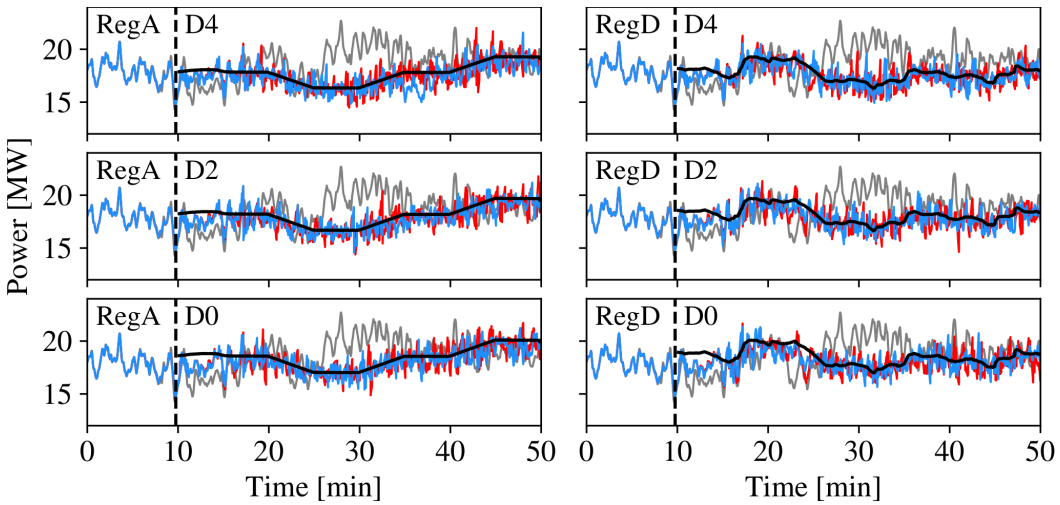

Fig. 5. Comparison of the power reference signal (black bold line), an uncontrolled LES case (gray line), the yaw and pitch controlled LES case (blue line), and the only pitch control LES case (red line). This figure shows comparisons for a representative RegA signal (left column), and a representative RegD signal (right column), for varying pitch derate values. The derate values are arranged by row, where the first row has a 4% derate, the second row has a 2% derate, and the third row has no derate.

applied to the wind farm and a sudden dip in the overall power caused by turbulent fluctuations, such that the pitch was unable to compensate for a short amount of time. Since the yaw control reacts on a slower timescale, it is unable to react to sudden changes due to turbulent fluctuations in the incoming wind. In this case, the pitch was also unable to compensate for this changing condition since it did not have enough control actuation available. In summary, we conclude that in these simulations, the yaw and pitch control offers a slight advantage over just the pitch control, and is able to actively leverage yaw to improve the control by a small but non-negligible amount.

2) A Greedy Control Case: In the previous studies presented here, the coefficient of thrust was initialized at $4/3$ to simulate standard operating conditions. However, as previously noted, this enables the thrust coefficient to have initial actuation authority, since the (local) thrust coefficient can still increase to its maximum theoretical value of 2. This means that the derates shown above are already derated from the average power when $C_T' = 4/3$ and not from the greedy power where $C_T' = 2$, i.e. building in an addition derate. We also wanted to investigate the effect of yaw on a wind farm operating in greedy control conditions where the thrust coefficient actuation is more limited.

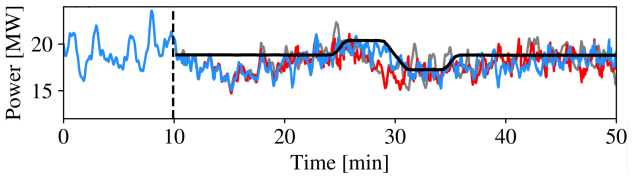

Fig. 6. Total power comparison for the case with a greedy initial condition and derated by 2% between the reference signal (bold black line), an uncontrolled LES case (gray line) [$RMSE_{nc} = 1.49$], the yaw and pitch controlled LES case (blue line) [$RMSE_{ypc} = 1.29$], and the only pitch controlled LES case (red line) [$RMSE_{ct} = 1.48$].

Figure 6 shows the total power of the yaw and pitch controlled LES case compared with the power reference signal (black), the only pitch control (red) and the uncontrolled LES case (grey) where the wind farm was initialized with $C_T' = 2$ (greedy control) but including a 2% derate. Initially, both control schemes clearly struggle to meet the power reference signal since there is not enough energy in the uncontrolled power to meet the demand. However, the yaw and pitch controller is able to leverage yaw to increase the power available, and is able to better meet the demand during the increase in the power reference signal, between 25 and 30 minutes. This is notable because both the uncontrolled LES case and the only pitch case are unable to meet this demand, suggesting that the yaw control was able to increase the power that could be extracted from the farm through wake steering during this time interval. These results show that the yaw control can be beneficial in power tracking particularly in reducing the required derate, which has economic implications.

IV. CONCLUSIONS

This paper describes and tests a coordinated pitch-yaw controller for active power tracking using wind farms. The controller leverages a dynamic yaw model that includes the spatial and temporal behavior of the wake due to yaw actions as it propagates through the farm. A novel power distribution scheme for pitch control actions enable the PI control to track the power signal with smaller derates than previous literature. Comparisons between this PI control for pitch and the integrated yaw-pitch control showed that coupling yaw with pitch control in the proposed control structure provides modest improvement in tracking secondary frequency regulation type signals for small turbine derates. However, the yaw augmentation was sometimes required to increase control authority in situations where the wind farm was close to its maximum power available (typically when the turbines were not derated). This work therefore provides a proof of

concept that dynamic yaw control can have benefits in power tracking, particularly in reducing the derates associated with revenue loss in the bulk power market and the probability of failure to meet the tracking goals. Reducing both of these items can improve the revenue potential of a farm providing frequency regulation services. Future work is needed to more comprehensively quantify the benefits of yaw in this application and to further investigate whether advances to the model predictive control framework for yaw can further improve performance.

ACKNOWLEDGEMENTS

G.M.S., C.M. and D.F.G. gratefully acknowledge partial funding support from the National Science Foundation (grant numbers DGE-1746891, CBET-1949778 and CMMI-1635430).

This work was coauthored by the National Renewable Energy Laboratory, operated by Alliance for Sustainable Energy, LLC, for the U.S. Department of Energy (DOE) under Contract No. DE-AC36-08GO28308. Funding provided by the U.S. Department of Energy Office of Energy Efficiency and Renewable Energy Wind Energy Technologies Office. The views expressed in the article do not necessarily represent the views of the DOE or the U.S. Government. The publisher, by accepting the article for publication, acknowledges that the U.S. Government retains a nonexclusive, paid-up, irrevocable, worldwide license to publish or reproduce the published form of this work, or allow others to do so, for U.S. Government purposes.

REFERENCES

[1] U.S. Energy Information Administration - EIA - independent statistics and analysis, "Electricity generation from wind," Mar 2022. [Online]. Available: https://www.eia.gov/energyexplained/wind/electricity-generation-from-wind.php

[2] C. R. Shapiro, G. M. Starke, and D. F. Gayme, "Turbulence and control of wind farms," *Annual Review of Control, Robotics, and Autonomous Systems*, 2021.

[3] S. Boersma, B. Doekemeijer, S. Siniscalchi-Minna, and J. van Wingerden, "A constrained wind farm controller providing secondary frequency regulation: An LES study," *Renewable Energy*, vol. 134, pp. 639–652, 2019.

[4] J.-W. van Wingerden, L. Pao, J. Aho, and P. Fleming, "Active power control of waked wind farms," *IFAC-PapersOnLine*, vol. 50, no. 1, pp. 4484–4491, 2017, 20th IFAC World Congress.

[5] J. Aho, A. Buckspan, J. Laks, P. Fleming, Y. Jeong, F. Dunne, M. Churchfield, L. Pao, and K. Johnson, "A tutorial of wind turbine control for supporting grid frequency through active power control," in *2012 American Control Conference (ACC)*. Piscataway, NJ: IEEE, 2012, pp. 3120–3131.

[6] C. R. Shapiro, P. Bauweraerts, J. Meyers, C. Meneveau, and D. F. Gayme, "Model-based receding horizon control of wind farms for secondary frequency regulation," *Wind Energy*, vol. 20, no. 7, pp. 1261–1275, 2017.

[7] P. Fleming, J. Aho, P. Gebraad, L. Pao, and Y. Zhang, "Computational fluid dynamics simulation study of active power control in wind plants," in *2016 American Control Conference (ACC)*. Piscataway, NJ: IEEE, jul 2016, pp. 1413–1420.

[8] C. R. Shapiro, J. Meyers, C. Meneveau, and D. F. Gayme, "Wind farms providing secondary frequency regulation: Evaluating the performance of model-based receding horizon control," *Wind Energy Science*, vol. 3, pp. 11–24, 2018.

[9] M. Vali, V. Petrović, G. Steinfeld, L. Y. Pao, and M. Kühn, "An active power control approach for wake-induced load alleviation in a fully developed wind farm boundary layer," *Wind Energy Science*, vol. 4, no. 1, pp. 139–161, mar 2019.

[10] H. Zhao, Q. Wu, Q. Guo, H. Sun, and Y. Xue, "Distributed model predictive control of a wind farm for optimal active power controlpart i: Clustering-based wind turbine model linearization," *IEEE Transactions on Sustainable Energy*, vol. 6, no. 3, pp. 831–839, 2015.

[11] S. Siniscalchi-Minna, F. D. Bianchi, and C. Ocampo-Martinez, "Predictive control of wind farms based on lexicographic minimizers for power reserve maximization," in *2018 Annual American Control Conference (ACC)*, 2018, pp. 701–706.

[12] L. Y. Pao and K. E. Johnson, "Control of wind turbines," *IEEE Control Systems*, vol. 31, no. 2, pp. 44–62, apr 2011.

[13] P. A. Fleming, A. Ning, P. M. O. Gebraad, and K. Dykes, "Wind plant system engineering through optimization of layout and yaw control," *Wind Energy*, vol. 19, no. 22, 3 2015.

[14] M. Bastankhah and F. Porté-Agel, "Wind farm power optimization via yaw angle control: A wind tunnel study," *J. Renew. Sustain. Ener.*, vol. 11, 2019.

[15] M. F. Howland, S. K. Lele, and J. O. Dabiri, "Wind farm power optimization through wake steering," *Proceedings of the National Academy of Sciences*, vol. 116, no. 29, pp. 14 495–14 500, 2019. [Online]. Available: https://www.pnas.org/content/116/29/14495

[16] P. M. O. Gebraad, F. W. Teeuwisse, J. W. van Wingerden, P. A. Fleming, S. D. Ruben, J. R. Marden, and L. Y. Pao, "Wind plant power optimization through yaw control using a parametric model for wake effects-a CFD simulation study," *Wind Energy*, vol. 19, no. 1, pp. 95–114, 2016.

[17] F. Mühle, J. Schottler, J. Bartl, R. Futrzynski, S. Evans, L. Bernini, P. Schito, M. Draper, A. Guggeri, E. Kleusberg, D. S. Henningson, M. Hölling, J. Peinke, M. S. Adaramola, and L. Sætran, "Blind test comparison on the wake behind a yawed wind turbine," *Wind Energy Science*, vol. 3, no. 2, pp. 883–903, 2018.

[18] P. Fleming, J. Annoni, J. J. Shah, L. Wang, S. Ananthan, Z. Zhang, K. Hutchings, P. Wang, W. Chen, and L. Chen, "Field test of wake steering at an offshore wind farm," *Wind Energy Science*, vol. 2, no. 1, pp. 229–239, 2017.

[19] P. Fleming, J. King, K. Dykes, E. Simley, J. Roadman, A. Scholbrock, P. Murphy, J. K. Lundquist, P. Moriarty, K. Fleming, J. van Dam, C. Bay, R. Mudafort, H. Lopez, J. Skopek, M. Scott, B. Ryan, C. Guernsey, and D. Brake, "Initial results from a field campaign of wake steering applied at a commercial wind farm – part 1," *Wind Energy Science*, vol. 4, no. 2, pp. 273–285, 2019.

[20] M. F. Howland, J. B. Quesada, J. J. P. Martínez, F. P. Larranaga, N. Yadav, J. S. Chawla, V. Sivaram, and J. O. Dabiri, "Collective wind farm operation based on a predictive model increases utility-scale energy production," *Nature Energy*, pp. 1315–1338, 2022.

[21] F. Campagnolo, V. Petrović, J. Schreiber, E. M. Nanos, A. Croce, and C. L. Bottasso, "Wind tunnel testing of a closed-loop wake deflection controller for wind farm power maximization," *Journal of Physics: Conference Series*, vol. 753, p. 032006, sep 2016.

[22] M. F. Howland, A. S. Ghate, S. K. Lele, and J. O. Dabiri, "Optimal closed-loop wake steering – part 1: Conventionally neutral atmospheric boundary layer conditions," *Wind Energy Science*, vol. 5, no. 4, pp. 1315–1338, 2020. [Online]. Available: https://wes.copernicus.org/articles/5/1315/2020/

[23] N. Cassamo and J.-W. van Wingerden, "Model predictive control for wake redirection in wind farms: A koopman dynamic mode decomposition approach," in *2021 American Control Conference (ACC)*. Piscataway, NJ: IEEE, May 2021, pp. 1772–1778.

[24] W. Munters and J. Meyers, "Dynamic strategies for yaw and induction control of wind farms based on large-eddy simulation and optimization," *Energies*, vol. 11, no. 1, pp. 1–32, 2018.

[25] G. M. Starke, C. Meneveau, J. R. King, and D. F. Gayme, "A dynamic model of wind turbine yaw for active farm control," *Preprint*, 2022.

[26] M. Bastankhah, C. R. Shapiro, S. Shamsoddin, D. F. Gayme, and C. Meneveau, "A vortex sheet based analytical model of the curled wake behind yawed wind turbines," p. A2, 2022.

[27] R. P. Brent, *Algorithms for minimization without derivatives*, ser. Prentice-Hall series in automatic computation. Prentice-Hall, 1972.

[28] W. H. Press, S. A. Teukolsky, W. T. Vetterling, and B. P. Flannery, *Numerical recipes: the art of scientific computing*, 3rd ed. Cambridge University Press, 2007.

[29] G. Van Rossum and F. L. Drake, *Python 3 Reference Manual*. Scotts Valley, CA: CreateSpace, 2009.

[30] R. J. A. M. Stevens, L. A. Martínez, and C. Meneveau, "Comparison of wind farm large eddy simulations using actuator disk and actuator

line models with wind tunnel experiments," *Renew. Energy*, vol. 116, no. Part A, pp. 470 – 478, 2018.
[31] R. J. Stevens, J. Graham, and C. Meneveau, "A concurrent precursor inflow method for large eddy simulations and applications to finite length wind farms," *Renewable Energy*, vol. 68, pp. 46–50, 2014.
[32] E. Bou-Zeid, C. Meneveau, and M. Parlange, "A scale-dependent lagrangian dynamic model for large eddy simulation of complex turbulent flows," *Physics of Fluids*, vol. 17, no. 2, p. 025105, 2005.
[33] M. Calaf, C. Meneveau, and J. Meyers, "Large eddy simulation study of fully developed wind-turbine array boundary layers," *Physics of Fluids*, vol. 22, no. 1, p. 015110, 2010.
[34] J. Meyers and C. Meneveau, "Large eddy simulations of large wind-turbine arrays in the atmospheric boundary layer," in *48th AIAA Aerospace Sciences Meeting*, 2010, p. 827.
[35] G. M. Starke, "Wind farm modeling for design and active power control of wind farms," Ph.D. dissertation, 2022.